

Defect Imaging using Sub-Sampled Array Data and Least Squares Migration

Katherine M. M. Tant
Department of Mathematics and
Statistics
University of Strathclyde
Glasgow, U.K.
katy.tant@strath.ac.uk

Carlos A. da Costa Filho^{1,2}
¹School of Geosciences
University of Edinburgh
Edinburgh, U.K.
andrew.curtis@ed.ac.uk
²CGG
Rio de Janeiro, Brazil
carlos.costa@cgg.com

Andrew Curtis^{1,2}
¹School of Geosciences
University of Edinburgh
Edinburgh, U.K.
andrew.curtis@ed.ac.uk
²Department of Geophysics
ETH Zurich
Zurich, Switzerland
curtisa@ethz.ch

Abstract—In ultrasonic phased array imaging, if the array element spacing is greater than half the wavelength, unwanted artefacts known as grating lobes can become prevalent and obscure signals arising from physical targets. This is problematic as use of dense, periodic arrays can result in large quantities of data and an acquisition time that is too lengthy for some applications. Thus, imaging algorithms which can act on sparsely collected data whilst retaining good image quality are highly desirable. Here we apply, for the first time to our knowledge, Least-Squares Migration (LSM), an imaging methodology originating within the seismology community, to sub-sampled ultrasonic array data, resulting in the attenuation of unwanted grating lobes. It is also shown that LSM can be used to obtain improved lateral resolution compared to that achieved by the Total Focusing Method, the current standard in ultrasonic NDT imaging.

Keywords—ulasonics, imaging, non-destructive testing, phased arrays

I. INTRODUCTION

In ultrasonic non-destructive testing (NDT), mechanical waves are injected into solid components and the wavefield which scatters from inhomogeneities in the medium is recorded. These data can then be used to generate an image of the component's interior without compromising its structural integrity. Ultrasonic NDT plays a particularly important role within safety-critical industries such as oil and gas, nuclear, and aerospace, where timely detection of structural weaknesses is vital. Ultrasonic linear phased arrays (which are capable of simultaneously transmitting and receiving ultrasonic signals across multiple piezoelectric transducers) allow NDT operators to perform fast and focused inspections with tailored ultrasonic beams at various angles and focal lengths [1]. A popular phased array data acquisition method is the Full Matrix Capture (FMC) technique, which facilitates the extraction of the maximum amount of information from a single array position [2]. It entails the sequential transmission of input waveforms from each of the of array elements whilst all elements simultaneously act as receivers. These FMC datasets can be post processed (using the Total Focusing method (TFM) for example [2]) to create high-resolution, focused images of internal defects.

Although FMC data acquisition allows us to detect and image defects accurately, it is limited by the requirement that, for an N element array, N independent transmissions are required [3]. Although increasing computational power means we can process increasingly larger FMC data sets in real time [4], the transmission time itself is constrained by the physics of wave propagation which ultimately makes FMC acquisition too slow for some applications.

One way to tackle this multiple transmission bottleneck is to implement plane wave imaging (PWI) which relies on simultaneous transmission across groups of neighboring elements, thus injecting more energy into the sample whilst reducing the number of independent transmissions [3]. The generation of these plane waves is based on Huygens principle, and so the array elements must be closely spaced to produce each plane wave front. Insufficient research has been carried out on the effects of an increased spacing between array elements (referred to as the array pitch) on the quality of PWI images.

Alternatively, sparsely populated arrays can be used to curtail data acquisition times whilst simultaneously minimizing hardware requirements. Random sparse arrays have already been investigated as a means to generating high quality images with fewer array elements. However, the optimal distribution of elements depends on each inspection scenario [5] e.g. a large gap within the array may mean an important aspect of the component's internal geometry is not sufficiently illuminated. Thus, sparse periodic arrays are an attractive option, allowing even illumination to be retained whilst reducing the number of transducers and time required. This is also desirable for the ongoing development of 2D arrays for volumetric imaging as typical phased array controllers only allow up to 256 channels; this limits the number of transducers into which sources can fire, thus making large and dense 2D arrays unfeasible due to the required channel count [6].

However, it is well known that if the array pitch is greater than half the wavelength λ , incomplete cancellation of the scattered waveforms leads to imaging artifacts known as grating lobes [6] which may obscure important signals arising from defects. This paper presents Least-Squares Migration (LSM), an imaging method originating from the

seismology community [7], as a candidate for diminishing the effects of grating lobes when imaging with periodic, sub-sampled data. We present a brief derivation of the method and examine three regularization approaches. The method is first validated using synthetic data from a finite element simulation of a linear phased array inspection of a steel block with embedded defects. In this case it is shown that use of the LSM significantly improves the lateral resolution when imaging two scatterers with sub-wavelength separation. The method is then applied to experimentally collected data where the array is sub-sampled so that the effective array pitch is greater than $\lambda/2$.

II. METHODOLOGY

In seismology, so-called migration methods are used to map scattered wave data recorded on the Earth's surface to points in the subsurface, allowing the construction of an image which represents the reflectivity of the region of interest. The benchmark NDT phased array imaging algorithm known as the Total Focusing Method (TFM) falls under the umbrella of Kirchhoff migration methods, which construct the image at a certain point by computing a weighted sum of all possible data which could have scattered from that point. This operation is linear and its adjoint is the forward modelling operator [7]. Therefore, since the migration operator used in TFM is not the true inverse of the forward modelling operator, but rather the adjoint, the reflectivity obtained with this method does not represent the correct reflectivity model. The least-squares migration (LSM) methodology iteratively approximates the true inverse, thus hopefully reconstructing an improved map of the component's reflectivity.

A. The Forward Model: Kirchhoff Demigration

We consider a homogeneous component with some reflectors (defects) embedded in its interior. We can then decompose our medium into a non-scattering background component (with reflectivity vector m_0) and a scattering component (with reflectivity vector m). To derive a linear relationship between the data and the component's reflectivity, we model the scattering of the wave field in the medium by L , a linear forward modelling operator constructed from Green's functions in the background medium. The main effect of this linearization is to disregard higher-order scattering in the medium. The collected ultrasonic phased array data d arising from the inspection of the component can then be written

$$d = Lm. \quad (1)$$

B. The Adjoint Model: Kirchhoff Migration

In Kirchhoff migration, each wave field recorded at each receiver placed on the surface of our sample is back-propagated to the region which we wish to image. This is achieved by representing the field at any point in our imaging domain as a weighted superposition of waves propagating from neighbouring points. Application of Kirchhoff migration requires a background model of the wave speed, which, within ultrasonic NDT, we typically assume to be constant. Let the Kirchhoff operator L' be adjoint to the linear forward modelling operator introduced in (1). We can then write

$$m_k = L'd, \quad (2)$$

where m_k is the Kirchhoff migrated map of reflectivity. Substituting (1) in (2), this can be rewritten

$$m_k = L'Lm. \quad (3)$$

If $L'L$ is the identity matrix, Kirchhoff migration faithfully reconstructs the true reflectivity map [7]. However, this is often not the case, as the standard TFM operator is not unitary, particularly when the acquisition setup is sparse. In this case, there is incomplete cancellation of the wave field and $L'L$ may introduce amplitude errors, shadow zones, frequency distortions and other imaging artefacts.

C. Least-Squares Migration

Least-squares migration tackles the challenge of correctly reconstructing m by minimising the problem

$$g(m) = \|Lm - d\|^2 + \|\Gamma m\|^2, \quad (4)$$

where Γ is a linear map introduced to regularise the problem (see Section II D). Equation (4) is then minimised at

$$m = (L'L + \Gamma'\Gamma)^{-1} L'd. \quad (5)$$

However, computing this inverse term directly is computationally expensive and so instead we solve

$$(L'L + \Gamma'\Gamma) m = m_k \quad (6)$$

using a matrix-free, iterative conjugate gradient scheme [8].

D. Regularisation

We introduce an operator Γ which penalizes unwanted features of the model, constrains the inversion and reduces the dimension of the solution space. In this paper we study three different approaches: $\Gamma = 0$ (no regularisation), $\Gamma = \mu I$ (minimum norm) and $\Gamma = \mu \Delta$ (minimum curvature), where I denotes the identity matrix, μ is a scaling factor and Δ is the discrete Laplacian. We select μ to equal 2% of the largest eigenvalue of $L'L$, computed using an Arnoldi iteration.

III. RESULTS

To demonstrate the improvements afforded by employment of the LSM, we first examine synthetic data generated by the finite element software PZFlex [9]. Within this software we model a 32-element linear phased array inspection of a steel sample measuring 20mm (depth) \times 52mm (length), with density of 7900kg/m³, and longitudinal wave speed of 5900m/s. For computational efficiency, the effects of the array were not included within the model. Instead, a pressure wavelet with centre frequency 1.5MHz was induced sequentially at 32 points (spaced 1mm apart to mimic the array pitch) along the top surface of the sample, and the scattered wave was recorded at the same 32 points simultaneously to generate the FMC dataset. The vertical boundaries of the model were assigned absorbing boundary conditions mimicking the inspection of a small section of a much larger sample, where diffractions from the edge of the sample are not recorded. Two circular voids with 1mm diameter were embedded 10mm below the array, spaced 1mm apart from each other (see Fig.1).

A. Improved Lateral Resolution

The inspection geometry shown in Fig. 1 allows us to compare the lateral resolution achieved using LSM to that of standard TFM. Fig. 2 shows the reconstruction of the two circular voids using the LSM implemented without regularization ($\Gamma = 0$), with a minimum norm regularization ($\Gamma = \mu I$), a minimum-curvature regularization ($\Gamma = \mu \Delta$), and finally using the standard TFM. Each image is plotted over a dynamic range of 20dB. It can be observed that these subwavelength scatterers with subwavelength spacing cannot

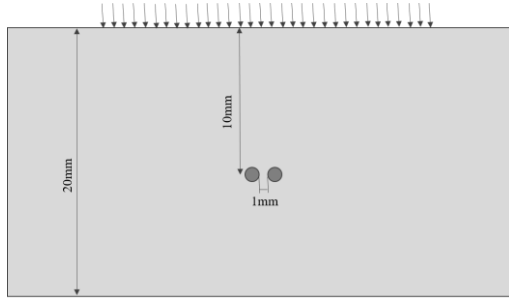


Fig. 1. Inspection geometry modelled in PZFlex to generate synthetic FMC data.

be independently resolved using standard TFM. However, in each case where LSM is employed, we observe a marked improvement in the separation of the two defects. In the case of no regularization, the image becomes pixelated and additional noise can be observed. Use of minimum curvature regularization results in the smoothest image, although the use of minimum-norm regularization suppresses the axial artefacts more successfully. This is reflected in the smaller residuals it produces, as shown in Fig. 3. Note that the shadows below the defect can be partially attributed to multiple scattering between the two defects [10] and the artefacts which appear above the defect are caused by insufficient damping of the input waveform. Note that if we convolve the forward modelling operator with the input wave

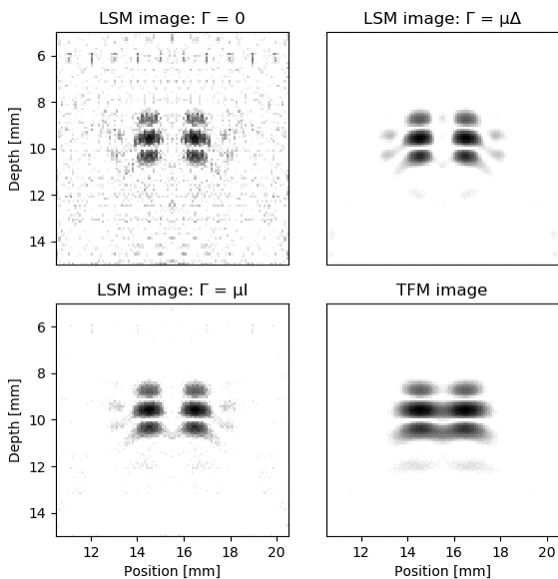


Fig. 2 Comparison of LSM implemented with no regularization ($\Gamma = 0$), minimum-norm regularization ($\Gamma = \mu I$), minimum-curvature regularization ($\Gamma = \mu \Delta$), and the standard TFM in imaging two 1mm diameter circular voids. All images are plotted over a dynamic range of 20dB.

these can be diminished. In this case, application of LSM with minimum-curvature regularization allows us to obtain good lateral resolution and suppression of these upper artefacts, although those caused by multiple scattering remain present (Fig. 4) and additional low level noise is observed. Application of the LSM with zero or minimum-norm regularization results in very noisy reconstructions and so are omitted for brevity.

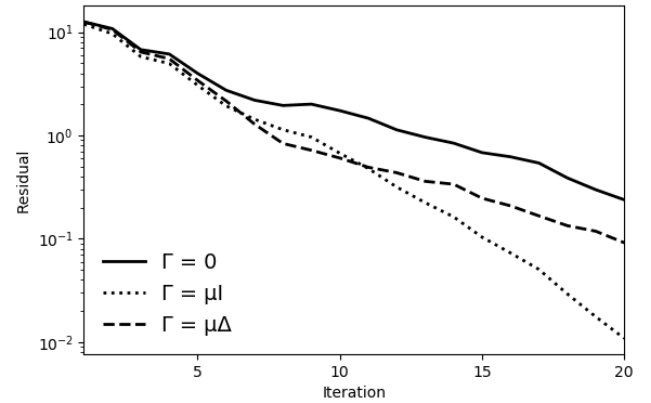


Fig. 3 Plot of the residuals as the conjugate gradient scheme is iterated within the LSM methodology for each of the three regularization approaches.

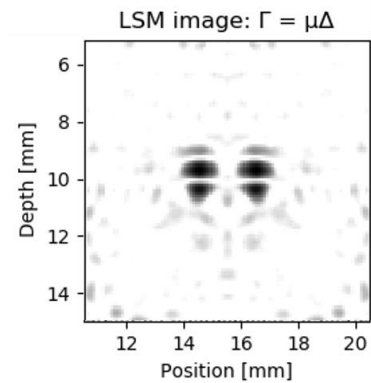


Fig. 4 Image of two 1mm diameter scatterers spaced 1mm apart achieved using LSM with minimum-curvature regularization where the forward modelling operator is convolved with the input waveform (plotted over a dynamic range of 20dB).

B. Suppression of Grating Lobes

To examine the ability of LSM to suppress grating lobes when the array is sub-sampled we apply the methodology to an experimentally collected FMC dataset. A 5MHz linear array (Vernon, France) with 128 elements, array pitch of 0.7mm and sample rate of 50MHz, controlled by the Zetec Dynaray® was used to inspect a steel block with a 3mm side drilled hole embedded 30mm below the centre of the array. The wave speed in the block was experimentally estimated as 5696m/s. The FMC data was sub-sampled by using only the data transmitted and recorded on every third array element. This was sufficient to observe significant grating lobes when the standard TFM algorithm was used to image the defect. Application of LSM with minimum-norm regularization and the TFM to this dataset is shown in Fig. 5 where the images are plotted over a dynamic range of 20dB (LSM with zero-regularization and minimum-curvature regularization were less effective in this case). It can be

observed that the grating lobes observed in the standard TFM image are suppressed in when LSM is employed.

C. Computational Cost

It has been shown here that the LSM performs well on sub-sampled array data, and thus presents an opportunity for NDT operators to reduce data acquisition times without compromising image quality. However, this comes at an added computational expense as LSM is an iterative technique. The times taken to generate the four images displayed in Fig. 2 are recorded in Table 1. These were generated using Julia v.0.7.0 on an Intel i5-7200 platform running at 2.5GHz, where the LSM was iterated 20 times in each case. Here, application of LSM takes approximately 60 times longer than the standard TFM. However, for applications such as railway track inspection where the data acquisition machinery is travelling at speeds of up to 32km/h [11] and the data is then post-processed offline, this trade off would be advantageous.

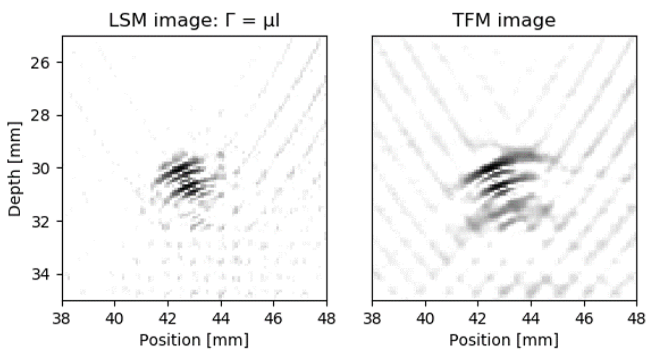


Fig. 5 Image of 3mm side drilled hole generated using subsampled data and both LSM with minimum-norm regularization and the TFM (plotted over a dynamic range of 20dB).

Table 1: Computation times for Fig. 2

Imaging Methodology	Time (s)
TFM	0.21
LSM: $\Gamma = 0$	12.97
LSM: $\Gamma = \mu I$	12.61
LSM: $\Gamma = \mu \Delta$	14.04

IV. CONCLUSIONS

Least-squares migration is presented here as alternative imaging methodology to the total focussing method for non-

destructive testing applications. Using a synthetic dataset, it was shown that the algorithm can provide better lateral resolution for sub-wavelength defects with sub-wavelength spacing. Three regularisation approaches were taken, and the minimum-norm and minimum-curvature regularisation techniques were shown to improve different aspects of the flaw reconstruction. Experimentally collected data was then used to examine the ability of LSM to suppress the effects of grating lobes when the array pitch violates the lower $\lambda/2$ bound. Only LSM with minimum-norm regularisation provided a significant improvement over the standard TFM. Future work will examine alternative regularisation approaches and optimisation of the scaling parameter μ , with a view to balancing image quality with number of iterations required.

V. REFERENCES

- [1] B. W. Drinkwater and P. D. Wilcox. "Ultrasonic arrays for non-destructive evaluation: A review." *NDT & E Int*, vol. 39, no. 7 pp. 525-541 2006.
- [2] C. Holmes, B. W. Drinkwater and P. D. Wilcox. "Post-processing of the full matrix of ultrasonic transmit-receive array data for non-destructive evaluation." *NDT & E Int*, vol. 38, no. 8, pp.701-711, 2005.
- [3] J. F. Cruza, J. Camacho, and C. Fritsch. "Plane-wave phase-coherence imaging for NDE." *NDT & E Int*, vol. 87, pp.31-37, 2017.
- [4] C. Wang, J. Mao, T. Leng, Z. Y. Zhuang, and X. M. Wang. "Efficient acceleration for total focusing method based on advanced parallel computing in FPGA." *The International Journal of Acoustics and Vibration*, vol 22, 2017.
- [5] P. Yang, B. Chen and K. R. Shi. "A novel method to design sparse linear arrays for ultrasonic phased array", *Ultrasonics*, vol. 44, pp.717-721, 2006
- [6] A. Volker and P. van Neer. "Imaging beyond aliasing." *AIP Conference Proceedings*, vol. 1706, no. 1, 2016.
- [7] T. Nemeth, C. Wu, and G. T. Schuster. "Least-squares migration of incomplete reflection data." *Geophysics*, vol. 64, no.1 pp.208-221, 1999.
- [8] M. R. Hestenes, and E. Stiefel. "Methods of Conjugate Gradients for Solving Linear Systems." *J Res Natl Bur Stand*, vol. 49, no.6, pp.409-436, 1952
- [9] OnScale, 6th Floor South Vincent Place, Glasgow, Scotland, G1 2ER.
- [10] C. Fan, M. Caleap, M. Pan and B. W. Drinkwater.. "A comparison between ultrasonic array beamforming and super resolution imaging algorithms for non-destructive evaluation." *Ultrasonics*, vol. 54, no.7 pp.1842-1850, 2014
- [11] R. Clark. "Rail flaw detection: overview and needs for future developments." *NDT & E International*, vol 37, no. 2, pp.111-118, 2004.